

# Case Based Reasoning in the Detection of Abnormalities in Retina Images: A Survey

Madhuparna Das Gupta, Sreeparna Banerjee

West Bengal University of Technology, Kolkata, West Bengal, India

**Abstract-** CBR is a paradigm that combines problem solving based on learning from past solutions. This subfield of AI has become increasingly popular in the last couple of decades especially in the medical domain as it emulates the doctors procedure that utilize past experience for diagnosis and treatment. In this paper an overview of CBR is presented, followed by a survey of CBR in the detection of abnormalities of the retina in fundus image.

**Keywords**—CBR; Retina Abnormalities; Similarity based retrieval;

## I. INTRODUCTION

Over the last few decades, Case Based Reasoning (CBR) has gained popularity as a problem solving and learning technique in Artificial Intelligence (AI). CBR is a paradigm based on the fact that similar problems have similar solutions. Doctors utilize past experiences for diagnosis and treatment which is the basic idea behind CBR. Hence CBR is mostly being used in the medical domain.

The advantages of CBR are manifold. Some of them include the fact that the knowledge acquisition task can be reduced and repetition of past mistakes and exploratory procedures are avoided. For domain that are not fully understood, yet possessing a small body of knowledge, CBR has proved to be particularly useful. Furthermore, since CBR draws from experiences from the past it learns over time.

The CBR procedure can be described by the CBR-cycle depicted in Fig.1 [1]. There are four essential steps involved as outlined below

- **Retrieve** similar cases to the problem description.
- **Reuse** a solution suggested by a similar case.
- **Revise** or adapt that solution to better fit the new problem if necessary.
- **Retain** the new solution once it has been confirmed or validated.

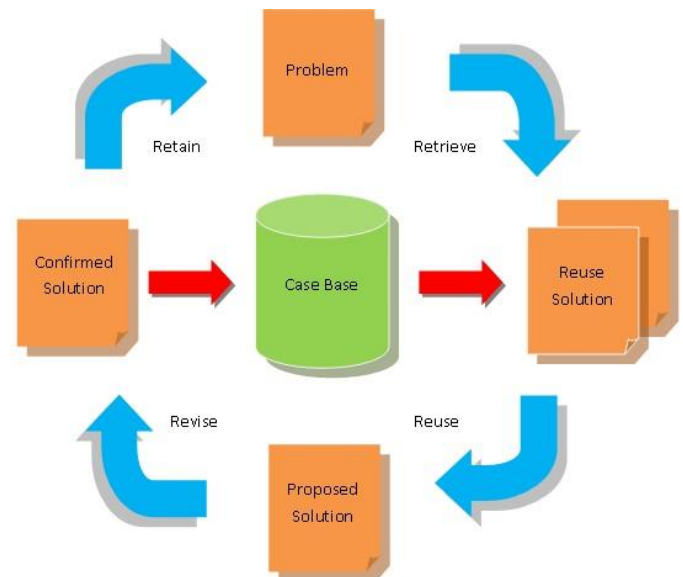


Fig.1: CBR Cycle [1]

Most of the applications of CBR in medicine are in the area of detection of retina abnormalities in fundus images in retina.

In the next section a brief review of the methodologies used in CBR will be given, followed by several sections on the various applications of CBR for abnormality detection in retina images.

A number of AI based methodologies have been employed to compare the attributes of the problems (or target) case with previous cases (prototype) stored in the case library. Some of these include Nearest neighbour (NN) [2], induction [2], fuzzy logic[3] and similarity based retrieval techniques from databases.

## II. METHODOLOGIES USED IN CBR

### A. CBR using Nearest Neighbour

Nearest Neighbour techniques are perhaps the most widely used technology in CBR and is provided by the majority of CBR tools [2]. In Nearest Neighbour algorithms the similarity of the problem (target) case to a case in the case-library for each case attribute is determined and this measure may be multiplied by a weighting factor. Then the sum of the similarity of all attributes is calculated to provide a measure of the similarity of that case in the library to the target case.

### B. CBR using Induction

Some of the powerful commercially available CBR tools use induction. Examples include Kate from AcknoSoft; ReCall from ISoft; CBR-Works from TecInno; and ReMind from Cognitive Systems [2]. Induction algorithms, such as ID3, build decision trees from case histories. The induction algorithms identify patterns amongst cases and partition the cases into clusters. Each cluster contains cases that are similar.

A requirement of induction is that one target case feature is defined (i.e. the feature that the algorithm will induce). Essentially the induction algorithms are being used as classifiers to cluster similar cases together.

### C. CBR using Fuzzy Logic

Fuzzy logics are a way of formalizing the symbolic processing of fuzzy linguistic terms, such as *excellent*, *good*, *fair* and *poor*, which are associated with differences in an attribute describing a feature [3]. Fuzzy logics intrinsically represent notions of similarity, since good is closer (more similar) to excellent than it is to poor. For CBR, a fuzzy preference function can be used to calculate the similarity of a single attribute of a case with the corresponding attribute of the target.

### D. CBR using Database Technology

Similarity based retrieval techniques for comparing images as well as meta data in databases are becoming increasingly popular [4]. The comparisons, Content or Features of the prototype present in case library databases are matched with those of the target cases. Matching criteria could be Decision Tree[5], **DSm&T**[6], Time series Analysis[7], Histogram based analysis[8].

## III. ABNORMALITIES IN RETINA

CBR has been applied to assist in the diagnosis and therapy planning of age related macular degeneration (AMD) and diabetic retinopathy (DR). In the following sections different types of abnormalities in retina are discussed.

### A. Age Related Macular Degeneration (AMD)

Age Related Macular Degeneration (AMD) is a disease associated with ageing, characterized by damage to the central part of the retina called macula.

There are two types of AMD, namely Dry AMD and Wet AMD.

- *Dry AMD*

Dry AMD[9] is characterized by multiple, medium to larger sized soft drusen within the macula. There are three stages of dry AMD: early, intermediate and advanced. The *early stage* of AMD is characterized by only a small number (less than 20) of moderate size drusen and patients may or may not notice any vision changes. The *intermediate stage* of AMD is characterized either by numerous (over 20) moderate sized soft drusen or several

large drusen. It is at the intermediate stage of AMD that most people notice changes in their vision. As AMD progresses into the *advanced stage*, large areas of damaged tissue called *geographic atrophy* form, causing central blind spots, an inability to read or even legal blindness.

- *Wet AMD*

Wet AMD [9], the more severe form is characterized by the growth of abnormal blood vessels below the retina called Choroidal Neovascularization, or CNV for short. Image analysis for dry and wet AMD constitute the detection of drusen (yellowish spots) as well as leaked blood vessel (red spots). Hanafi et al [7] have used time series analysis to perform CBR in the detection of AMD. Authors here described an approach to Case Based Reasoning (CBR) for image categorisation. The technique is founded on a time series analysis mechanism whereby images are represented as time series and compared using time series similarity techniques. This paper explores two mechanisms where images can be represented as time series (curves). The first takes into account the entire image while the second is directed at some specific feature within the image. The choice of images is partially dependent on the nature of the application. If the content of the entire image is important or if there is no single defining feature, then the first should be adopted. The second approach is only applicable if there is some feature that exists across the image set that is significant with respect to a particular application. Once a time series representation has been adopted some similarity checking mechanisms are required.

### B. Diabetic Retinopathy (DR)

Diabetic retinopathy consists of a variety of morphological lesions in the retinal fundus related to disturbances in retinal blood flow [10]. Diabetic Retinopathy is a medical condition where the retina is damaged because fluid leaks from blood vessels into the retina. The presence of haemorrhages in the retina is the earliest symptom of diabetic retinopathy. The number and shape of haemorrhages is used to indicate the severity of the disease.

Diabetic retinopathy is diagnosed by fundus photography. The manifestation of DR are MA (blood spots), Exudates (both hard and soft) and later neovascularisation.

Hemorrhages and microaneurysms are the first clinically observable lesions indicating diabetic retinopathy. Therefore, their detection is very important for a diabetic retinopathy screening system. Early automated hemorrhage detection can help reduce the incidence of blindness.

- *Microaneurysm and Hemorrhages*

MA constitutes one of the earliest signs of MA caused due to blood vessel leakage and appear in the macular area and retinal periphery. Generally, the density of red dots reflects the density of the retinal capillary system which is highest in the macular area apart from the foveal avascular

zone, and decreases towards the retinal periphery. By definition, the diameter of a microaneurysm is less than 100  $\mu\text{m}$ , but most frequently the diameter of the lesion is not larger than 10–20  $\mu\text{m}$  [10]. The differentiation of a microaneurysm from a small well defined dot haemorrhage cannot be done on the basis of ophthalmoscopy alone, but requires fluorescein angiography by which a microaneurysm fills with fluorescein, whereas a haemorrhage remains dark.

### Ensemble creation

In this section, the ensemble creation approach is based on creating a set of <preprocessing method, candidate extractor> or shortly <PP, CE> pairs. Simulated Annealing has also been used to find optimal pairs. In [5], authors present a Case Based Reasoning (CBR) system for the retrieval of medical cases made up of a series of images with contextual information (such as the patient age, sex and medical history). When designing a CBR system to retrieve such cases, several problems arise: we have to aggregate heterogeneous variables (images, nominal and continuous variables), and moreover, we sometimes have to deal with missing information. Decision trees (generally used for classification) are well suited to solve both these problems. So a retrieval framework from decision trees is derived [4], which are well suited to process heterogeneous and incomplete information. In [4] it emerges that a retrieval system based on several trees is also more accurate than system based on single tree. Two novel information fusion methods are proposed in [12]. In the first method, the degrees of match are fused by the Bayesian network itself. In the second method, they are fused by the Dezert-Smarandache theory. The proposed methods were applied to two heterogeneous medical databases, a diabetic retinopathy database and a mammography screening database, for computer aided diagnosis.

- *Exudates*

Retinal **exudates** are precipitations of plasma protein that have leaked from the retinal vessels [10]. The typical 'hard' exudate appears as a sharply delimited whitish lesion in the surrounding reddish retina. The typical exudate has approximately the size of a microaneurysm, but the lesion may expand and merge with neighbouring lesions to form larger conglomerates of exudates. Soft exudates are called wool spots. Exudates may occur as solitary lesions, in groups, or arranged in a circinate pattern concentrically around a single leakage point to form so-called exudate rings. Hard exudates develop later than microaneurysms and haemorrhages, but typically show the same spatial pattern of distribution with the lesions starting temporally from the fovea from where they may spread to other parts of the macular area. The density of hard exudates decreases from the vascular arcades and the lesion is typically absent from the retinal periphery.

### 1) Microaneurysm Detection

Computer-aided MA detection [13] is based on the detailed analysis of digital fundus images. MAs appear as small circular dark spots on the surface of the retina. The detection of MAs is still not sufficiently reliable, as it is hard to distinguish them from certain parts of the vascular system. This problem increases the number of false candidates that naturally deteriorates the overall accuracy of the detectors. To overcome this difficulty, the creation of an ensemble of <preprocessing method, candidate extractor> pairs using state-of-the-art individual algorithms is proposed [11, 14]. Some preprocessing methods, which can be used before executing MA extraction are described below.

#### Walter-Klein contrast enhancement

This preprocessing algorithm described in [15] aims to enhance the contrast of fundus images by applying a gray level transformation using the following factor,

$$f' = \frac{1}{2} \frac{(f'_{max} - f'_{min})}{(\mu - f'_{min})^r} \cdot (f - f'_{min})^r + f'_{min}, \quad f \leq \mu \quad (1)$$

$$= -\frac{1}{2} \frac{(f'_{max} - f'_{min})}{(\mu - f'_{max})^r} \cdot (f - f'_{max})^r + f'_{max}, \quad f \geq \mu \quad (2)$$

where  $\{f'_{min}, \dots, f'_{max}\}$ ,  $\{f_{min}, \dots, f_{max}\}$  are the intensity levels of the original and the enhanced image, respectively,  $\mu$  is the mean value of the original grayscale image and  $r \in \mathbb{R}$  is a transition parameter.

#### Contrast Limited Adaptive Histogram Equalization

Contrast limited adaptive histogram equalization (CLAHE) is a popular technique in biomedical image processing, since it is very effective in making the usually interesting salient parts more visible [16]. The image is split into disjoint regions, and in each region a local histogram equalization is applied. Then, the boundaries between the regions are eliminated with a bilinear interpolation.

#### Vessel Removal and Extrapolation

The effect of processing images with the complete vessel system being removed. The missing parts are extrapolated to fill in the holes caused by the removal using the inpainting algorithm presented in [17]. MAs appearing near vessels become more easily detectable in this way.

#### Illumination Equalization

The preprocessing method described in [18] aims to reduce the vignetting effect caused by uneven

illumination of retinal images. Each pixel intensity is set according to the following formula:

$$f' = f + \mu_d - \mu_l \quad (2)$$

Where  $f$ ,  $f'$  are the original and the new pixel intensity values, respectively,  $\mu_d$  is the desired average intensity, and  $\mu_l$  is the local average intensity. MAs appearing on the border of the retina are enhanced by this step.

#### Grey World Normalization (GN)

Grey World Normalization technique is proposed in [19] which uses the following formula,

$$r^{new} = \frac{r}{R_{avg}}, g^{new} = \frac{g}{G_{avg}}, b^{new} = \frac{b}{B_{avg}}$$

where (r, g, b) are the original intensity values,  $R_{avg}$ ,  $G_{avg}$  and  $B_{avg}$  are the average intensity values in each band and ( $r^{new}$ ,  $g^{new}$ ,  $b^{new}$ ) are the new values, respectively.

#### Division by an over-smoothed (DS)

The mean of the intensity values is computed within a window according to [18]. The original intensity value is divided by the mean value of its neighbourhood.

#### Morphological contrast enhancement (MC)

Morphological opening and closing are applied in [18]. Then the new intensity values are subtracted from the original intensity values multiplied by three.

#### Background subtraction (BS)

The background is estimated by computing the mean of the intensity values within a  $W_1 \times W_1$  window. The mean of the previously calculated values are computed in a  $W_2 \times W_2$  window are subtracted from the intensity value of each pixel [18].

#### No Preprocessing

The results of the candidate extractors obtained for the original images without any preprocessing are also considered. That is, a "no preprocessing" operation is formally considered, as well. Equations

##### 2) Microaneurysm candidate extractors

Candidate extraction is a process which aims to spot objects in the image showing MA like characteristics [13]. Individual MA detectors follow their own way to extract MA candidates.

Walter et al. [20] have proposed a candidate extractor method using greyscale diameter closing candidate. Candidates appear as sufficiently small dark patterns on the green channel of the image. The final MA candidates are the remaining objects in the image after executing this operation.

#### Spencer-Frame [21] [22]

In the approach of **Spencer-Frame** the actual candidate extraction is accomplished by subtracting the maximum of multiple morphological top-hat transformations. For this step, twelve rotated structuring elements are used with a radial resolution of  $15^\circ$ . Then, the resulting image is subtracted from  $i_{sc}$  to remove the largest components from the image. In the next step, a 2D Gaussian matched filter is applied on the obtained image. Finally, the resulting image is thresholded and a region growing step is applied.

#### Circular Hough-transformation [23]

It performs Candidate extraction by detecting circles on the images in this circular Hough transformation method. The radius of the circles are set according to the size of MAs from a training set.

In the method of **Lazar et al. [24]**, Pixel-wise cross-section profiles with multiple orientations are used to construct a multi-directional height map. This map assigns a set of height values that describe the distinction of the pixel from its surroundings in a particular direction. In a modified multilevel attribute opening step a score map is constructed, from which the MAs are extracted by thresholding.

In the method of **Zhang et al. [25]**, multi-scale correlation filtering and dynamic thresholding is performed. For the first task, it uses five Gaussian masks with different sigmas. The maximum coefficients from the five responses are then combined.

#### Optimal morphology (Om) [26]

Sopharak et al. proposed a method based on optimally adjusted morphological operations. The optic disc is removed, and Otsu's algorithm is used to threshold during the detection process.

#### Coarse-to-fine (CTF) [27]

This technique is based on morphological operations and H-maxima transform. Contrast enhancement on L channel is applied after the image is converted from ROB to LUV color space.

**Fuzzy C-Means clustering (FCM)**

Sopharak et al. [28] proposed several candidate extraction method which include morphological operations for optic disk removal coupled with otsu’s algorithm for segmentation, fuzzy c-means clustering [14], and Naïve Bayes [29]. Other methods include CTF [27], Split and Merge [30]. Sopharak et al. proposed another method in [10] using fuzzy c-means clustering in order to determine whether a pixel is exudates or non-exudate. They used four features to obtain a coarse segmentation result. Then, morphological operations are applied to refine the segmentation result.

**Naïve Bayes (NB) [29]**

Sopharak et al. proposed an exudate extractor algorithm which used a pixel-based classification. Five features based on a classic machine learning approach are extracted to classify pixels.

**Split-and-merge (SMF, SMC) [30]**

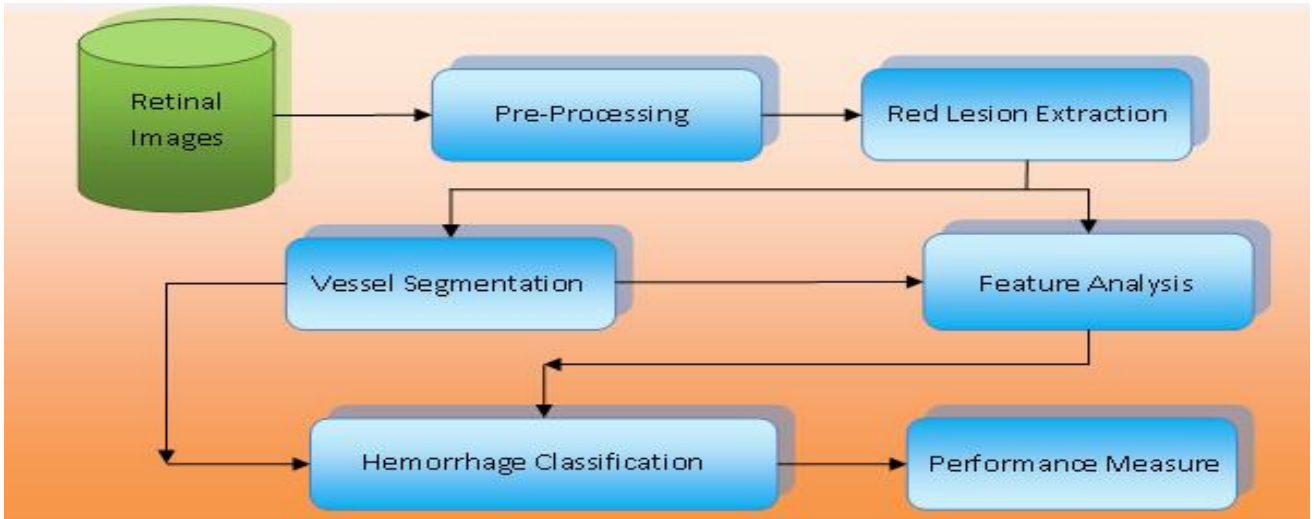
The exudate detection was divided into two steps in this method. In the coarse step (SMC), the high local variances between the exudates and background are found. The algorithm splits the images into disjoint regions and then merges them in

database. Finally, the rest of the pixels are classified by their related properties.

- *Hemorrhage Detection*

Hemorrhage detection can be divided into 2 consequent stages: Red lesion candidate extraction and Classification. After the image preprocessing stage to reduce noise and improve contrast, the red areas of the picture are considered as the candidates for red lesion. Vessel Segmentation algorithms are used to extract blood vessels from candidates, thereby reducing false detection, followed by feature selection and extraction for hemorrhage detection. The classification algorithm is applied to categorize these features into the hemorrhage group (abnormal) and not hemorrhage group (normal). Overall processes for detection of hemorrhages are concluded in Fig. 2[32]. Detection of haemorrhages is generally carried out using morphological method [32], a collection of techniques used for extracting image components. Several methods are outlined below.

Soft computing method such as NN [33], multilayer perception, radial basis function, Support Vector Machine and majority voting were also used to detect red lesion [34]. Authors in [35, 36, and 37] have used region growing segmentation techniques to extract red lesions. An inverse method utilizing the background image of healthy areas for detection of diabetic retinopathy lesions has been reported in Kose et al. [38].



the fine step (SMF) if they were enough homogenous. A histogram-based thresholding was used for the merged parts as adaptive thresholding.

**Hard-Exudates (HE)**

The method used in [31] is pixel-based classification, but the training database is extracted from the currently analyzed image. First, the algorithm detects the sure exudates and uses them as positive pixels to set the training

IV. CONCLUSION

In this paper we have presented an overview of CBR as increasingly popular paradigm in AI, based on the intuition that problems tend to recur and so past solutions provide insights for solving present problems.

A survey of several applications of CBR in the diagnosis of retina abnormalities from fundus images has been conducted.

Abnormalities in the retina include AMD and DR. AMD can further be classified as Dry AMD, the more prevalent form and Wet AMD, which is more severe. The former is characterized by drusen which is yellowish deposits of extra cellular material, 88888 there are additional broken blood vessels present in the later case. CBR of retina images with AMD has been performed using a time series analysis based procedure. DR, another common abnormality of retina is manifested in images through microaneurysm and hard and soft exudates. The earliest symptom of DR is MA which shows up as red spots in the retina due to focal dilations of capillaries. Hard exudates are yellowish flecks which are lipid deposits caused by leakage from damaged capillaries. Soft exudates or cotton wool spots are nerve fibre layer infarcts, which are white in colour. CBR methods for detecting MA in DR images include the application of AI techniques like Decision Trees, Bayesian Network, Dezert Smarandache Theory. Some image preprocessing and MA extraction techniques used for these retina images have also been discussed. An overview of hemorrhage detection techniques for retina images are also discussed.

From a study of CBR in retina abnormality detection it is found that CBR is particularly useful for domains that are not well understood yet possessing a confined body of knowledge. Therefore it is hoped that in the future CBR can be applied to other problem areas as well.

#### ACKNOWLEDGEMENT

The authors wish to acknowledge the research grant from the Department of Biotechnology, Govt. of India (Proj. No. **BT/PR4256/BID/7/393/2012, Dt. 02/08/2012**).

#### V. REFERENCES

- [1] Aamodt, E. Plaza. Case-Based Reasoning: Foundational Issues, Methodological Variations and System Approaches. *AI Communications*, 17(1), 1994.
- [2] I. Watson, Applying Case-based Reasoning: Techniques for Enterprise Systems, Morgan Kaufmann, CA, USA, 1997.
- [3] J. Mendel, Fuzzy logic systems for engineering: a tutorial, *Proc. IEEE* 83 (3) (1995).
- [4] M Das Gupta, S Banerjee, "Similarity based retrieval in case based reasoning for analysis of medical images", In the proceedings of ICIPACV 2014, March 24-25, Turkey, Istanbul
- [5] Gw'eno'le Quellec, Mathieu Lamard, Lynda Bekri, Guy Cazuguel, B'eatrice Cochener, Christian Roux, —Multimedia medical case retrieval using decision trees, 29th Annual International Conference of the IEEE EMBS, Lyon, France, August 23-26, 2007.
- [6] F. Smarandache and J. Dezert, Advances and Applications of DSMT for Information Fusion I. American Research Press Rehoboth, 2004, <http://fs.gallup.unm.edu/DSmT-book1.pdf>.
- [7] Ashraf Elsayed, Mohd Hanafi Ahmad Hijazi, Frans Coenen, Marta Garcia-Finana, Vanessa Sluming, Yalin Zheng, —Image Categorisation Using Time Series Case Based Reasoning, International conference on case based reasoning (ICCB 2011), London, UK, Springer 2011, pp. 423-436.
- [8] Hijazi, M.H.A., Coenen, F., Zheng, Y.: Image Classification using Histograms and Time Series Analysis: A Study of Age-related Macular Degeneration (AMD) Screening in Retina Image Data. In: Perner, P. (eds) *ICDM 2010*. LNCS, vol. 6171, pp. 197-209 (2010)
- [9] <http://www.retinaeye.com>
- [10] Toke Bek, "Clinical Presentations and Pathological Correlates of Retinopathy", Hammes H-P, Porta M (eds): *Experimental Approaches to Diabetic Retinopathy*. Front Diabetes. Basel, Karger, 2010, vol 20, pp 1–19
- [11] B'alint Antal\*, Andr'as Hajdu, "An Ensemble-Based System for Microaneurysm Detection and Diabetic Retinopathy Grading" *IEEE TRANSACTIONS ON BIOMEDICAL ENGINEERING*, VOL. 59, NO. 6, JUNE 2012, pp. 1720-1726.
- [12] Gw'eno'le Quellec, Mathieu Lamard, Guy Cazuguel, Member, IEEE, Christian Roux, Fellow Member, IEEE and B'eatrice Cochener, —Case Retrieval in Medical Databases by Fusing Heterogeneous Information, *IEEE Transaction on medical imaging* 2010, pp.1-11.
- [13] B'alint Antal, Andr'as Hajdu, "AN ENSEMBLE-BASED MICROANEURYSM DETECTOR FOR RETINAL IMAGES" 2011 18th IEEE International Conference on Image Processing.
- [14] Brigitta Nagy, Balazs Harangi, B'alint Antal, Andr'as Hajdu, "Ensemble-based exudate detection in color fundus Images", 7th International Symposium on Image and Signal Processing and Analysis (ISPA 2011) September 4-6, 2011, Dubrovnik, Croatia, pp. 700-703.
- [15] T. Walter and J. Klein, "Automatic detection of microaneurysms in color fundus images of the human retina by means of the bounding box closing," *Lecture Notes in Computer Science*, vol. 2526, pp. 210–220, 2002.
- [16] K. Zuiderveld, "Contrast limited adaptive histogram equalization," *Graphics Gems*, vol. 4, pp. 474–485, 1994.
- [17] S. Ravishankar, A. Jain, and A. Mittal, "Automated feature extraction for early detection of diabetic retinopathy in fundus images," in *Proc. IEEE Conf. Comput. Vision Pattern Recog.*, 2009, pp. 210–217.
- [18] A. A. Youssif, A. Z. Ghalwash, and A. S. Ghoneim, "Comparative study of contrast enhancement and illumination equalization methods for retinal vasculature segmentation," in *Proc. Cairo Int. Biomed. Eng. Conf.*, 2006, pp. 21–24.
- [19] A. A. Youssif, A. Z. Ghalwash, and A. S. Ghoneim, "A Comparative Evaluation of Preprocessing Methods for Automatic Detection of Retinal Anatomy", *Proceedings of the Fifth International Conference on Informatics & Systems (INFOS 2007)*, pp. 24-30, 2007
- [20] T. Walter, P. Massin, A. Arginay, R. Ordonez, C. Jeulin, and J. C. Klein, "Automatic detection of microaneurysms in color fundus images," *Medical Image Analysis*, vol. 11, pp. 555–566, 2007.
- [21] T. Spencer, J. A. Olson, K. C. McHardy, P. F. Sharp, and J. V. Forrester, "An image-processing strategy for the segmentation and quantification of microaneurysms in fluorescein angiograms of the ocular fundus," *Computers and Biomedical Research*, vol. 29, pp. 284–302, May 1996.
- [22] J. Frame, P. E. Udrill, M. J. Cree, J. A. Olson, K. C. McHardy, P. F. Sharp, and J. Forrester, "A comparison of computer based classification methods applied to the detection of microaneurysms in ophthalmic fluorescein angiograms," *Computers in Biology and Medicine*, vol. 28, pp. 225–238, 1998.
- [23] S. Abdelazeem, "Microaneurysm detection using vessels removal and circular hough transform," *Proceedings of the Nineteenth National Radio Science Conference*, pp. 421 – 426, 2002.

- [24] Lazar, B. Antal, and A. Hajdu, "Microaneurysm detection in digital fundus images," Tech. Rep. 2010/14(387), University of Debrecen, Hungary, 2010.
- [25] B. Zhang, X. Wu, J. You, Q. Li, and F. Karray, "Detection of microaneurysms using multi-scale correlation coefficients," *Pattern Recogn.*, vol. 43, no. 6, pp. 2237–2248, 2010.
- [26] Sopharak, B. Uyyanonvara S. Barman and T. H. Williamson, "Automatic detection of diabetic retinopathy exudates from non-dilated retinal images using mathematical morphology methods", *Computerized Medical Imaging and Graphics*, vol. 32, no. 8, pp. 720-727, 2008.
- [27] D. Welfer, J. Scharcanski and D. R. Marinho, "A coarse-to-fine strategy for automatically detecting exudates in color eye fundus images", *Computerized Medical Imaging and Graphics*, vol. 34, no. 3, pp. 228-235, 2010.
- [28] Sopharak, B. Uyyanonvara and S. Barman, "Automatic exudate detection from nondilated diabetic retinopathy retinal images using fuzzy c-means clustering", *Sensors*, vol. 9, no. 3, pp. 2148-2161, 2009.
- [29] Sopharak, M. N. Dailey, B. Uyyanonvara, S. Barman, T. Williamson, K. T. Nwe and Y. A. Moe, "Machine learning approach to automatic exudates detection in retinal images from diabetic patients", *Journal of Modern Optics*, vol. 57, no. 2, pp. 124-135, 2010.
- [30] H. F. Jaafar, A. K. Nandi and W. Al-Nuaimy, "Detection of exudates in retinal images using a pure splitting technique", *Engineering in Medicine and Biology Society (EMBC 2010)*, pp. 6745-6748, 2010.
- [31] C. I. Sanchez, R. Hornero, M. I. Lopez, M. Aboy, J. Poza and D. Abasolo, "A novel automatic image processing algorithm for detection of hard exudates based on retinal image analysis", *Medical Engineering & Physics*, vol 30, no. 3, pp. 350-357, 2008.
- [32] Parisut Jitpakdee, Pakinee Aimmanee, Bunyarit Uyyanonvara, "A Survey on Hemorrhage Detection in Diabetic Retinopathy Retinal Images", *IEEE conference*, 2012.
- [33] Gardner G, Keating O, Williamson TH, Ell AT., "Automatic detection of diabetic retinopathy using an artificial neural network: a screening tool", *Br J Ophthalmol*, vol. 80, pp. 940-4, 1996.
- [34] Garcia M, Lopez MI, Alvarez D, Hornero R., "Assessment of four neural network based classifiers to automatically detect red lesions in retinal images", *Med Eng Phys*. 2010 Dec;32(10):1085-93. Epub 2010.
- [35] C. Marino, E. Ares, M.G. Penedo, M. Ortega, N. Barreira, F. Gomez Ulla, "Automated Three Stage Red Lesions Detection In Digital Color Fundus Images", *WSEAS Transactions on Computers*, vol. 7, pp. 207- 215, 2008.
- [36] Sinthanayothin C, Boyce JF, Williamson TH, Cook HL, Mensah E, Lal S, et al., "Automated detection of diabetic retinopathy on digital fundus images", *Diabet Med.*, vol. 19, pp. 105-12, 2002.
- [37] J.P. Bae, K.G. Kim, H.C. Kang, C.B. Jeong, K.H. Park, and J. Hwang "A Study on Hemorrhage Detection Using Hybrid Method in Fundus Images", presented at *J. Digital Imaging*, pp. 394-404, 2011.
- [38] Kose C, Sevik U, Ikiba C, Erdol H., "Simple methods for segmentation and measurement of diabetic retinopathy lesions in retinal fundus images", *Comput Methods Programs Biomed.*, 20 II.